

# Statistical analysis of the fracture behaviour of porous ceramic Raschig rings

J.M. Villora, P. Callejas, M.F. Barba, C. Baudín\*

*Instituto de Cerámica y Vidrio, CSIC—Campus de Cantoblanco, Camino de Valdelatas s/n, 28049 Madrid, Spain*

Received 6 December 2002; received in revised form 27 February 2003; accepted 6 April 2003

## Abstract

Microstructural control during processing is necessary to assure uniform performance of random packed columns filled with ceramic Raschig rings. In this work, the statistical analysis of the fracture strength of three series of Raschig rings fabricated using three different green processes, uniaxial pressing, extrusion and slip casting, is proposed as a method of comparing the reliability of the three processes. The rings were prepared from industrial and urban wastes and contained hydroxyapatite as agent for the ionic exchange that leads to the immobilisation of heavy metals. Strength values were determined by the diametric compression of ring test and results were analysed using Weibull statistics. Results were correlated with scanning microscope observations of fracture surfaces. Simple monomodal two parameter Weibull statistics have been demonstrated to be suitable to analyse the fracture behaviour of the rings. From the stand point of strength reliability, extrusion is proposed as the most adequate green forming method. © 2003 Elsevier Ltd. All rights reserved.

**Keywords:** Apatites; Failure analysis; Fracture; Functional applications; Porosity; Shaping; Testing

## 1. Introduction

The random packed columns filled with Raschig rings are widely used for waste-water treatment. Ceramic materials are preferred as fillers due to their capability of standing aggressive environments and the possibility of fabricating highly porous pieces with sufficient strength. The effectiveness of the rings is a function, not only of their shape, which determines the packing efficiency as well as the packing surface area, but also, of the material properties such as porosity and specific surface area. Therefore, microstructural control during processing is necessary to get reliable performance in use. On the other hand, one single ring has to present sufficient mechanical properties to support impact during the filling of the column as well as the load of the rings located over it during use. Moreover, regardless of the specific mechanical solicitations during use, highly porous ceramic Raschig rings can

provide interesting data about the mechanical behaviour of highly porous materials.

The most used green processing methods to fabricate these rings at industrial level are extrusion and uniaxial pressing. An alternative way for the industrial production of ceramic pieces is from slip cast green bodies; in principle, this processing route would also be adequate to shape Raschig rings.

Hydroxyapatite has been proposed to be responsible for the ionic exchange that leads to the immobilisation of heavy metals from waste-waters.<sup>1–7</sup> However, it is not possible to obtain sintered pieces of this phase alone, due to its decomposition at temperatures higher than 1000 °C, and the mechanical properties of hydroxyapatite are extremely low. Stability of hydroxyapatite can be increased by adding an excess of CaO to the material<sup>4,8</sup> and the mechanical properties can be improved by the presence of SiO<sub>2</sub>. Considering the components of urban and industrial wastes such as animal bones, waste diatom filters from beer companies and paper industry sludges, compositions in the system P<sub>2</sub>O<sub>5</sub>–CaO–SiO<sub>2</sub>–Al<sub>2</sub>O<sub>3</sub>–(Alk)<sub>2</sub>O to obtain hydroxyapatite and crystalline SiO<sub>2</sub> in the final material can be formulated.<sup>9</sup>

\* Corresponding author. Tel.: +34-91-735-5840; fax: +34-91-735-5843.

E-mail address: [cbaudin@icv.csic.es](mailto:cbaudin@icv.csic.es) (C. Baudín).

In this work, the statistical analysis of the fracture strength of three series of Raschig rings, prepared from industrial and urban wastes by using the three green processes mentioned above, is proposed as a method to compare the reliability of the three processes. Fracture behaviour was characterised in terms of the stress to fracture of “as fabricated” rings placed under diametrical compression loading (“Brittle Ring Test”<sup>10</sup>). Simple Weibull statistics<sup>11</sup> were applied to the obtained results and the suitability of this method for characterising the fracture behaviour was analysed. The parameters of the monomodal probability function were used to compare the relative reliability of the three processes. The simple loading method used can also be routinely used for quality control of the similarly shaped pieces during fabrication.

### 1.1. Mechanical testing and analysis

When the ring is placed under diametrical compression,<sup>10</sup> maximum tensile stresses are developed on the inner periphery of the annulus in the loading plane. Tension, to a lesser degree, is also developed on the transverse diameter of the outer periphery. Compressive stresses are developed on the opposite sides of the neutral axes of these same points; however, these stresses may be neglected since failure will be caused by the maximum tensile stress. To evaluate stress, the empirical equation proposed and tested for a number of ceramics by Frocht<sup>10</sup> was selected. The failure stress,  $\sigma$ , of the ring due to the action of the maximum tensile stresses is given by:

$$\sigma = \frac{P \cdot K_4}{(D_o - D_i) \cdot t} \quad (1)$$

where  $P$  is the load to failure,  $D_o$ ,  $D_i$  and  $t$  are the outside diameter, the inside diameter and the width of the ring, respectively, and  $K_4$  is the stress constant, which is a function of the ratio  $D_i/D_o$ .

Linear elastic mechanics shows that for brittle materials fracture is determined by the presence of flaws, that act as stress concentrators; this stands for dense as well as for highly porous materials. Concerning critical flaws, the effect of pores has been analysed as stress concentrators on a thin flaw localised in the solid away from the pores, or as an integral part of the flaws considering that fracture occurs by the extension of cracks located at the cavity surface.<sup>12–14</sup> In highly porous materials (porosity > 40%<sup>15</sup>), where pores are closely spaced, subcritical crack linking can occur prior to overall failure. The fracture stress is then given by the stress to propagate the critical flaw generated by subcritical flaw linking.<sup>12,16</sup> In principle, failure of highly porous materials should be described by the probability function proposed by Weibull,<sup>11</sup> that describes failure occurring from critical flaws. Nevertheless, very little data have been reported for porous materials.<sup>12,14,16,17</sup>

Nanjagud et al.<sup>17</sup> have used this analysis to describe materials containing pores due to incomplete sintering (porosity ≈ 10–40%) and Pernot et al.<sup>12</sup> to characterise the strength distribution of porous phosphate glass ceramics, (porosity ≈ 50–75%). Both studies demonstrated the suitability of the simplest form of the Weibull function, therefore, in principle, this function could be applied to highly porous ceramic Raschig rings.

The Weibull distribution can be expressed as a cumulative distribution:

$$P_f(\sigma) = 1 - \exp\left(\frac{-(\sigma - \sigma_t)^m}{\sigma_\phi^m}\right) \quad (2)$$

where  $P_f(\sigma)$  is the probability of failure at a stress  $\sigma$ ,  $\sigma_0$  is a scaling constant,  $\sigma_t$  is the threshold stress below which no failure occurs in the material, that practically can be taken as zero for brittle ceramics, and  $m$  is the Weibull modulus. The scaling constant  $\sigma_0$ , usually called characteristic strength, corresponds to the stress at which the probability of failure is 63.2%.<sup>18</sup> The Weibull modulus controls the shape of the curve, being larger as the degree of scatter of the strength values decreases. Therefore, larger values of  $m$  describe more reliable materials.

To evaluate  $P_f$ , the following equation was used:

$$P_f = \frac{n}{N + 1} \quad (3)$$

where  $N$  is the total number of specimens tested and  $n$  is the specimen rank in ascending order of failure stress. This equation gives an unbiased estimate of the  $n$ th failure and is recommended when the number of specimens tested is between 20 and 30.<sup>18–20</sup>

## 2. Experimental

Animal bones, waste diatom filters from beer companies and paper industry sludges were used as raw materials. The chemical composition of the mixture (wt.% = P<sub>2</sub>O<sub>5</sub>: 14.6; CaO: 29.3; SiO<sub>2</sub>: 50.0; MgO: 0.64; Al<sub>2</sub>O<sub>3</sub>: 2.19; Fe<sub>2</sub>O<sub>3</sub>: 0.82; K<sub>2</sub>O: 0.68; Na<sub>2</sub>O: 1.76) was adjusted to obtain hydroxyapatite and crystalline silica in the sintered materials.

Homogeneous mixture of the raw materials with appropriate granulometry was obtained by sieving (< 0.5 mm) and attrition milling with alumina balls (30 min). Medium particle size after milling was about 6 μm. From this powder, three series of green bodies were prepared using the above mentioned shaping methods: uniaxial pressing, extrusion and slip casting.

A stable suspension was prepared using a solid/liquid ratio 50/50 and 0.25 wt.% of deflocculant (sodium polyacrylate: Dispex N-40, Allied Colloids, USA), using a magnetic stirrer. Subsequently, 2 wt.% of binder

(Carboxymethyl cellulose: Optapix C 1000 G, Zschimmer & Schwarz, Germany) was added and homogenised. This slip was poured into plaster moulds of 10 mm diameter and 200 mm length. For a wall thickness of about 2.2 mm, formation time was 15 min.

The paste used for extrusion was prepared using 2.5 wt.% of a plasticizer (polysaccharide: Zusoplast PS-1: Zschimmer & Schwarz, Germany) with binding properties and 40% humidity. A laboratory manual vertical extrusion machine with a die of 5 mm internal diameter and 9.5 mm external diameter was used to form tubes of 200 mm length.

For uniaxial pressing, 10 wt.% of water and 1 wt.% of binder (polyvinyl alcohol: Optapix PAF 35, Zschimmer & Schwarz, Germany) were used. The moulds, used in an industrial machine press (RC2-Spain) sized 9.3 mm external diameter and 5.4 mm internal diameter; the pressing conditions were fixed to obtain rings of exterior diameter equal to height.

All green bodies were dried and sintered using the same sintering schedule (heating and cooling rate: 6 °C/min, 1150 °C—1 h) in an electric furnace (SATER, Spain) in air. This sintering temperature was chosen, from dynamic sintering data and heating microscope observations, to avoid extensive glass in the materials. As will be seen in which follows, the fired densities reached by the rings and, consequently, the dimensions, were a function of the green processing method. Therefore, in order to obtain sintered cylinders with similar external diameters, the dimension of the external diameter of the pressing mould, the extrusion die and the slip casting mould were adjusted. Cylinders of similar weight (0.35–0.48 g), external diameter ( $\approx 8$  mm) and width ( $\approx 8$  mm) were obtained as final test pieces.

Bulk density of the green and sintered bodies was determined by the Archimedes method using Hg. True densities of the sintered rings were determined in an He pycnometer (Multipycnometer, QuantaChrome, USA). Total porosity in the sintered materials was calculated from bulk and true density values.

Specific surface areas were determined by the BET method (Monosorb Analyzer MS-13, QuantaChrome, USA), using liquid N<sub>2</sub> as adsorbate.

For the diametrical compression tests, the rings were loaded using steel compression plates in a universal testing machine (Microtest, Spain) at a relatively high deformation rate (10 mm/min) in order to simulate impact. Additional tests were performed using 1 mm/min.

### 3. Results and discussion

#### 3.1. Materials

Physical and geometrical characteristics of the rings obtained following the three green processing methods

are summarised in Table 1. The largest green density values correspond to the pressed materials, followed by the extruded ones, and the lowest values are those for the slip cast rings. In agreement with the more effective packing revealed by green density values, sintered densities follow the same trend. As the sintering temperature used was the maximum permitted to avoid extensive glass formation in the materials, no further optimisation of this temperature to reach higher sintering levels depending on the green processing method was permitted. Therefore, differences between the sintering densities should be considered as directly related to the green processing method.

Specific surface area is significantly lower for the pressed rings whereas, in spite of bulk density differences, specific surfaces areas are practically coincidental for the series prepared by extrusion and slip casting. For the same packing of equal shape and size rings, effective contact surface for ionic exchange will increase with specific surface area values, therefore, in terms of this parameter, extrusion and slip casting seem to be the most adequate green processing methods.

External diameters are practically coincidental for the three series of rings, as expected from the fabrication parameters (mould and die diameters), and significant differences exist between the internal diameters, which are much larger for the pressed rings, in agreement with the larger shrinkage that occurs during sintering.

#### 3.2. Mechanical behaviour

In Fig. 1a the characteristic shape of the load-displacement curves of tests performed at low deformation rate (1 mm/min) is shown. In all cases, fracture occurred in two steps, being the second load peak higher than the first one. When the test was stopped after the first load peak, the test pieces were broken across the diameter parallel to the loading plane into two “c rings”, revealing that the first peak corresponded to the fracture starting from the inner periphery of the annulus in the loading plane, accordingly with the stress distribution described above. The second load peak corresponded to the fracture of the two remaining “c rings”, due to the tension developed on the transverse diameter of their outer periphery. The change in the slope of the load-displacement curves of samples

Table 1  
Physical and geometrical characteristics of the studied Raschig rings

	Pressing	Extrusion	Slip
Green density (g/cm <sup>3</sup> )	1.4 $\pm$ 0.1	1.0 $\pm$ 0.1	0.8 $\pm$ 0.1
Bulk density (g/cm <sup>3</sup> )	1.84 $\pm$ 0.04	1.4 $\pm$ 0.1	1.1 $\pm$ 0.1
Porosity (vol.%)	34	47	60
Specific surface area (m <sup>2</sup> /g)	0.2 $\pm$ 0.1	0.6 $\pm$ 0.1	0.7 $\pm$ 0.1
External diameter (mm)	8.0 $\pm$ 0.2	7.96 $\pm$ 0.08	8.0 $\pm$ 0.4
Internal diameter (mm)	4.60 $\pm$ 0.09	3.9 $\pm$ 0.1	3.4 $\pm$ 0.4

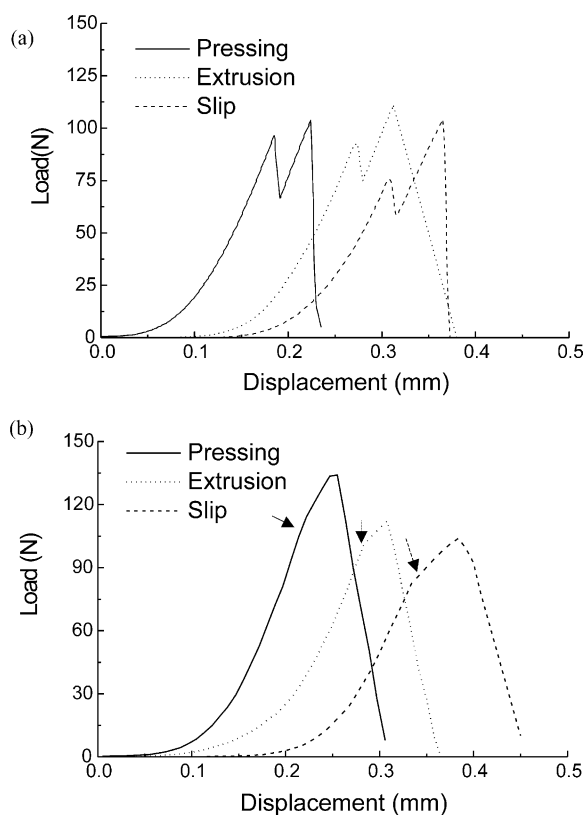


Fig. 1. Characteristic shape of the load–displacement curves for tests of the three series of materials: uniaxially pressed, extruded and slip cast. (a) Tests performed at low loading rate (1 mm/min). Two clearly differentiated load peaks are observed. (b) Tests performed at high loading rate (10 mm/min). Arrows show the first breaking load.

tested at high deformation rate (10 mm/min, Fig. 1b) allows differentiation of the two load values corresponding to the two fracture stages described above.

As the first load corresponds to the first failure of the cylinders, the statistical analysis was realised in terms of the stress calculated, from this value and the dimensions of the specimens (Table 1), using Eq. (1). The stress constant  $K_4$  was taken from the empirical relationships between  $K_4$  and  $D_i/D_o$  given by Frocht.<sup>10</sup> From the dimensions of the specimens (Table 1), the ratios are 0.6, 0.5 and 0.4, for pressing, extrusion and slip, respectively, which lie in the part of the Frocht's curve experimentally tested for a number of ceramics ( $D_i/D_o=0.3$ – $0.8$ ) and correspond to  $K_4$  values of 8.7, 7 and 6 for pressing, extrusion and slip, respectively.

The  $\text{Ln}(\text{Ln})$  plots for the experimental values of stress and the probabilities of failure [Eq. (3)], shown in Fig. 2, were used to evaluate graphically the constants  $m$  and  $\sigma_0$ . Table 2 summarises the Weibull parameters corresponding to the linear adjustments. In Fig. 3 the probability of failure as a function of stress, calculated from the Weibull parameters (Table 2), is depicted together with the experimental values and the corresponding probability of failure calculated using Eq. (3). The three series of rings show good fits ( $R=0.98$ – $0.99$ ) for

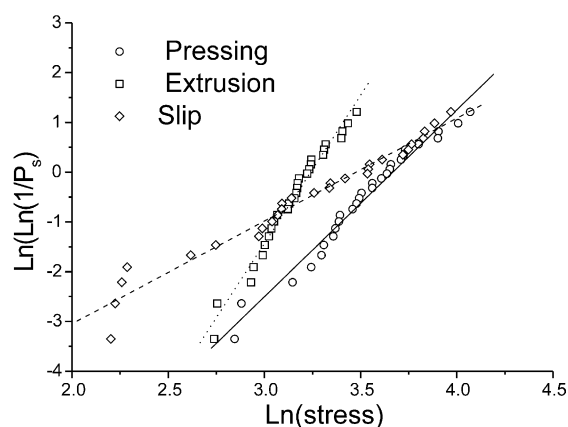


Fig. 2. Weibull plots for the three series of specimens. The processing route is signalled in the plot.  $P_s = 1 - P_f$  is the probability of survival at the corresponding stress.

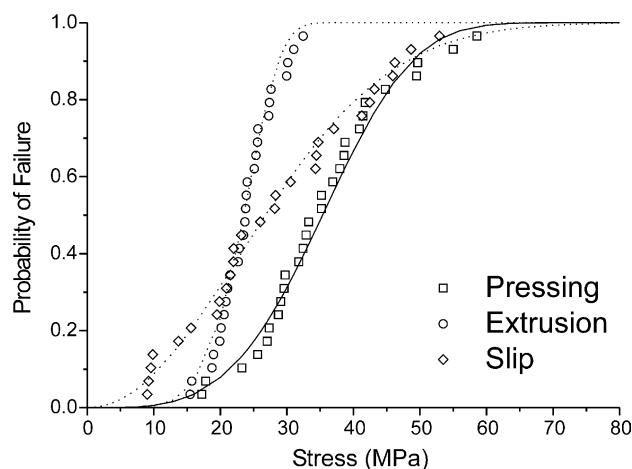


Fig. 3. Probability of failure as a function of stress (lines), calculated from the Weibull parameters (Table 2), compared with the experimental values (symbols) and the corresponding probability of failure calculated using Eq. (3). The processing route is signalled in the plot.

Table 2  
Parameters of the Weibull distributions

Processing method	$m$	Characteristic strength (MPa)	$R$	Average strength (MPa)
Uniaxial pressing	3.7	39	0.99	35
Extrusion	6.0	25	0.99	24
Slip casting	2.0	32	0.98	27
Slip casting (24 samples)	2.9	34	0.98	28

monomodal distributions and, accordingly, a good adjustment is obtained between the experimental values and the calculated curves (Fig. 3).

Characteristic defects observed in the rings fabricated by the three green processing methods were pores and pore arrangements as those shown in Fig. 4a–c, that were large ( $\approx 200 \mu\text{m}$ ) and uniform in size and elongated shape for the extruded cylinders (Fig. 4b). In the slip cast samples, pores were smaller than in the extruded



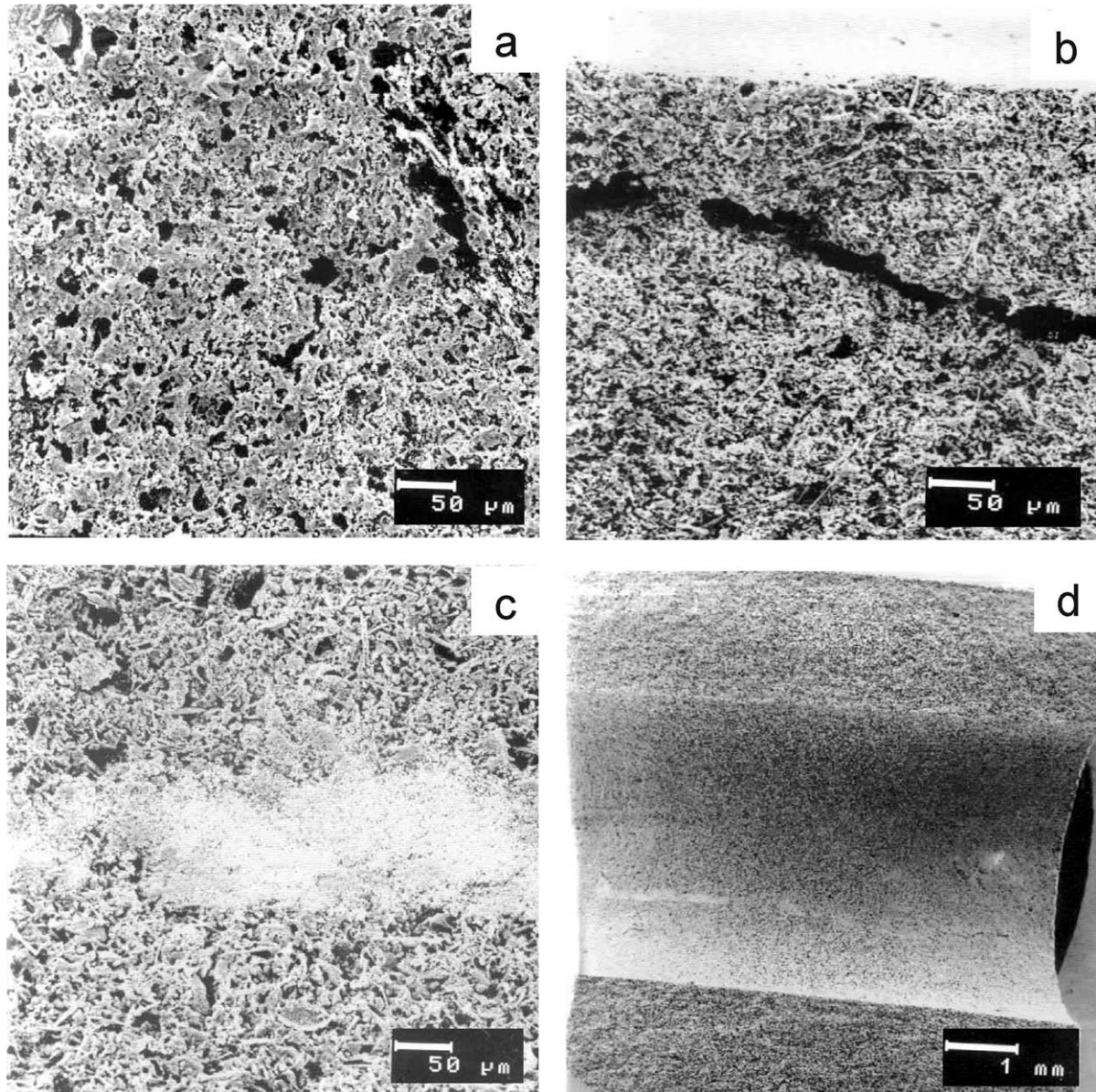


Fig. 4. Characteristic defects observed in the rings fabricated by the three green processing methods. SEM micrographs of fracture surfaces. (a) Uniaxially pressed rings. Pores and pore arrangements of variable shape and size. (b) Extruded rings. Large ( $\approx 200 \mu\text{m}$ ) and uniform in size and shape pores and pore arrangements. (c) Slip cast rings. Small and uniform pores and highly dense linear area. (d) Slip cast rings. Large ( $> 500 \mu\text{m}$ ) linear defects constituted of pores and highly dense linear areas.

ones and presented variable size and shape (Fig. 4c). In the pressed samples (Fig. 4a), pores were the smallest and had variable size.

However, in the slip cast cylinders large ( $> 400 \mu\text{m}$ ) linear defects constituted of pores (Fig. 4d) and highly dense areas (Fig. 4c–d) were also observed. The largest of these linear defects, that practically run along the whole width of the rings (Fig. 4d), would be responsible for the lowest strength values, as observed in the four samples that presented similar and extremely low strengths (9 MPa). As these linear defects are probably due to discontinuities originated in the inner part of the green compacts during the removal of the slip excess

from the plaster mould, in principle, they could be avoided industrially. Therefore, a new Weibull adjustment was performed eliminating the above mentioned strength values to characterise the slip casting process. In this case average strength slightly increases due to the elimination of the lowest strength values. Even though the Weibull modulus is larger (Table 2, Slip casting, 24 samples) it is still lower than those obtained for the pressed and extruded series of rings.

The characteristics of the Weibull distributions (Table 2) are in agreement with the microstructural observations (Fig. 4a–c). The extruded rings, with large and uniform defects, exhibit the highest value of Weibull modulus but

low average strength. The pressed ones, with the smallest defects of variable size, present a lower modulus but the largest average strength. The lowest value of the modulus and the intermediate average strength correspond to the slip cast cylinders, in which defects with variable size and shape were found.

The facts that good fits are found for monomodal Weibull distributions and that results are in agreement with the microstructural observations, demonstrate that, even for the high levels of porosity considered here (34–60 vol.%), fracture of the materials is well described by the “weakest link” theory, as proved by other authors for highly porous materials.<sup>12,17</sup>

In summary, from the Weibull analysis performed here, extrusion appears as the most adequate of the three methods studied, as the microstructure of the rings will be more homogeneous and, consequently, the operation of the column will be more reliable than when the rings are prepared using the other two considered methods. Moreover, this method leads to reasonable good values of specific surface area when compared with those obtained for the uniaxially pressed and slip cast rings.

#### 4. Conclusions

The microstructural characteristics and mechanical behaviour of three series of ceramic Raschig rings prepared by uniaxial pressing, extrusion and slip casting have been characterised.

From the stand point of specific surface area values, extrusion and slip casting appear as more adequate green forming methods than uniaxial pressing. In the case of extrusion, the high value of the specific surface area is accompanied by intermediate density values.

Simple monomodal two parameter Weibull statistics are suitable to analyse the fracture behaviour of the rings under diametric compression.

From the stand point of strength reliability, extrusion is the most adequate green forming method.

#### Acknowledgements

The authors acknowledge CICYT for the economical support of this project and Mahou company for the supply of used diatoms.

#### References

1. Ma, Q. Y., Logan, T. J. and Traina, S. J., Effects of  $\text{NO}_3^-$ ,  $\text{Cl}^-$ ,  $\text{F}^-$ ,  $\text{SO}_4^{2-}$ , and  $\text{CO}_3^{2-}$  on  $\text{Pb}^{2+}$  immobilization by hydroxyapatite. *Environ. Sci. Technol.*, 1994, **28**(3), 408–418.
2. Ma, Q. Y., Logan, T. J., Traina, S. J. and Ryan, J. A., Effects of

- aqueous Al, Cd, Cu, Fe(II), Ni, and Zn on Pb immobilization by hydroxyapatite. *Environ. Sci. Technol.*, 1994, **28**(7), 1219–1228.
3. Suzuki, S., Fuzita, T., Maruyama, T., Takahashi, M. and Hiki-chi, Y., Cation-exchange characteristics of sintered hydroxyapatite in the strongly acidic region. *J. Am. Ceram. Soc.*, 1993, **76**(6), 1638–1640.
4. Suzuki, S., Itoh, K., Ohgaki, M., Ohtani, M. and Ozawa, M., Preparation of sintered filter for ion exchange by a doctor blade method with aqueous slurries of needlelike hydroxyapatite. *Ceram. Int.*, 1999, **25**, 287–291.
5. Binner, J. G. P. and Reichert, J., Hydroxyapatite filters for the removal of heavy metals ions from aqueous solutions. *Br. Ceram. Proc.*, 1996, **55**, 63–78.
6. Reichert, J. and Binner, J. G. P., An evaluation of hydroxyapatite-based filters for removal of heavy metal ions from aqueous solutions. *J. Mater. Sci.*, 1996, **31**, 1231–1241.
7. Furuta, S., Katsuki, H. and Komarneni, S., Removal of lead ions using porous hydroxyapatite monoliths synthesized from gypsum waste. *J. Ceram. Soc. Japan*, 2000, **108**(3), 315–317.
8. Villora, J. M., Callejas, P. and Barba, M. F., Métodos de síntesis y comportamiento térmico del Hidroxiapatito. *Bol. Soc. Esp. Ceram. Vidrio*, 2002, **41**(5), 443–450.
9. Villora, J.M., Callejas, P. and Barba, M.F., Processing of highly porous hydroxyapatite from waste raw materials. In *Proceedings of the 7th conference & exhibition of the European Ceramic society*, ed. Trans Tech Publications, Key Engineering Materials, Switzerland, 2002, pp. 895–898.
10. Bortz, S.A. and Lund, H.H., The brittle ring test. In *The proceedings of a conference conducted by the School of Engineering and the College Extension Division, North Carlonina State College in cooperation with the Office and Ordnance Research*, ed. Interscience Publishers, New York-London, 1961, pp. 383–406.
11. Weibull, W., A statistical distribution function of wide applicability. *J. Appl. Mech.*, 1951, **293–297**.
12. Pernot, F., Etienne, P., Boschet, F. and Datas, L., Weibull parameters and the tensile strength of porous phosphate glass-ceramics. *J. Am. Ceram. Soc.*, 1999, **82**(3), 641–648.
13. Evans, A. G., Biswas, D. R. and Fulrath, R. M., Some effects of cavities on the fracture of ceramics: I, cylindrical cavities. *J. Am. Ceram. Soc.*, 1979, **62**(1–2), 95–100.
14. Evans, A. G., Biswas, D. R. and Fulrath, R. M., Some effects of cavities on the fracture of ceramics: II, spherical cavities. *J. Am. Ceram. Soc.*, 1979, **62**(1–2), 101–109.
15. Rice, R. W., Relation of tensile strength-porosity effects in ceramics to porosity dependence of Young's modulus and fracture energy, porosity character and grain size. *Mater. Sci. Eng.*, 1989, **A112**, 215–224.
16. Evans, A. G. and Tapin, G., Effects of microstructure on the stress to propagate inherent flaws. *Proc. Br. Ceram. Soc.*, 1972, **20**(6), 275–297.
17. Nanjangud, S. C., Brezny, R. and Green, D. J., Strength and Young's modulus behaviour of a partially sintered porous alumina. *J. Am. Ceram. Soc.*, 1995, **78**(1), 266–268.
18. Osborne, B. K., *Reliability of a Flint Clay Hollow Sphere as Determined by Weibull Statistical Analysis of Failure Loads*. MS thesis, University of Missouri, Rolla, 1991.
19. Bergman, B., On the estimation of the Weibull modulus. *J. Mater. Sci. Lett.*, 1984, **689–690**.
20. Sullivan, J. D. and Lauzon, P. H., Experimental probability estimators for Weibull plots. *J. Mater. Sci. Letters*, 1986, **5**, 1245–1247.